Synthesis, biological evaluation and molecular modeling study of 5-trifluoromethyl-Δ2-pyrazoline and isomeric 5/3-trifluoromethylpyrazole derivatives as anti-inflammatory agents

ARTICLE *in* EUROPEAN JOURNAL OF MEDICINAL CHEMISTRY · OCTOBER 2013

Impact Factor: 3.45 · DOI: 10.1016/j.ejmech.2013.09.052 · Source: PubMed

6 AUTHORS, INCLUDING:

Ranjana Aggarwal
Kurukshetra University
59 PUBLICATIONS **571** CITATIONS
SEE PROFILE

Anshul Bansal
S. A. JAIN COLLEGE, AMBALA CITY
4 PUBLICATIONS **21** CITATIONS
SEE PROFILE

Brendan Kelly
Stanford University
14 PUBLICATIONS **79** CITATIONS
SEE PROFILE

Dhirender Kaushik
Ch. Bansi Lal University, Bhiwani
55 PUBLICATIONS **278** CITATIONS
SEE PROFILE

European Journal of Medicinal Chemistry 70 (2013) 350–357

Contents lists available at ScienceDirect

European Journal of Medicinal Chemistry

journal homepage: http://www.elsevier.com/locate/ejmech

Original article

Synthesis, biological evaluation and molecular modeling study of 5-trifluoromethyl-Δ^2-pyrazoline and isomeric 5/3-trifluoromethylpyrazole derivatives as anti-inflammatory agents

Ranjana Aggarwal [a,*], Anshul Bansal [a], Isabel Rozas [b], Brendan Kelly [b], Pawan Kaushik [c], Dhirender Kaushik [c]

[a] Department of Chemistry, Kurukshetra University, Kurukshetra, Haryana 136 119, India
[b] School of Chemistry, Trinity Biomedical Sciences Institute, Trinity College Dublin, 154-160 Pearse St., Dublin 2, Ireland
[c] Institute of Pharmaceutical Sciences, Kurukshetra University, Kurukshetra 136 119, India

ARTICLE INFO

Article history:
Received 4 May 2013
Received in revised form
23 September 2013
Accepted 28 September 2013
Available online 7 October 2013

Keywords:
5-Trifluoromethyl-Δ^2-pyrazolines
3-Trifluoromethylpyrazoles
5-Trifluoromethylpyrazoles
Anti-inflammatory activity
COX-2
Docking

ABSTRACT

Searching for new anti-inflammatory agents, we have prepared a series of potential COX-2 inhibitors, 1-(4,6-dimethylpyrimidin-2-yl)-5-hydroxy-5-trifluoromethyl-Δ^2-pyrazolines (3) and 1-(4,6-dimethylpyrimidin-2-yl)-3-trifluoromethylpyrazoles (4), by refluxing 2-hydrazino-4,6-dimethylpyrimidine (1) with a number of trifluoromethyl-β-diketones (2) in ethanol. Further dehydration of compounds (3) to the corresponding 1-(4,6-dimethylpyrimidin-2-yl)-5-trifluoromethylpyrazoles (5) was also achieved. Fifteen of these compounds were screened for their anti-inflammatory activity using the carrageenan-induced rat paw edema assay. While all the compounds exhibited significant anti-inflammatory activity (47–76%) as compared to indomethacin (78%), 3-trifluoromethylpyrazoles (4) were found to be the most effective agents (62–76%). To rationalize this anti-inflammatory activity, docking experiments molecular dynamics simulations were performed to study the ability of these compounds to bind into the active site of the COX-2 enzyme.

1. Introduction

Inflammation plays a fundamental role in the immune response of the human body to microbes, injury or trauma. Recent studies have demonstrated that inflammation is key not only in infection and cancer but also to autoimmune diseases, such as rheumatoid arthritis, multiple sclerosis, type I diabetes and Crohn's disease, or certain neuro-degenerative conditions [1–4].

One of the most important factors in the inflammatory process is the generation of prostaglandins which are produced by the action of cyclooxygenase (COX) on arachidonic acid. For that reason, this enzymatic system became a popular target for the development of anti-inflammatory drugs such as the non-steroidal anti-inflammatory drugs or NSAIDs which exert their activity by inhibiting COX, thus preventing the synthesis of prostaglandins [5].

From the known forms of COX, it seems that COX-2 is the one responsible of prostaglandin production in inflammatory conditions. Thus, COX-2 inhibitors have been prepared for the treatment of chronic inflammatory diseases like rheumatoid and osteoarthritis, and many of them, such as celecoxib or SC-588 (Fig. 1), have a similar core, the trifluoromethylpyrazole system [6].

Several pyrazole derivatives have been reported to possess pharmacological activity as anti-inflammatory agents [7–9]. Further, incorporation of the lipophilic trifluoromethyl group on pyrazole ring exerts a variety of dramatic effects on the pharmacological properties of the molecule making its partition into cell membranes much easier and hence increasing the selectivity, efficacy and bioavailability [10]. Also pyrimidine derivatives, the fundamental building blocks for DNA and RNA, have attracted a great deal of attention over many years due to their broad bioactivities, including antitumor [11,12], antimicrobial [13], or anti-inflammatory [14].

In view of these observations and continuing with our work related to the synthesis and spectroscopic and biological studies of trifluoromethylpyrazoles [15–18], we have prepared and evaluated

* Corresponding author. Tel.: +91 1744238734; fax: +91 1744238277.
E-mail addresses: ranjana67in@yahoo.com, ranjanaaggarwal67@gmail.com (R. Aggarwal).

0223-5234/$ – see front matter © 2013 Elsevier Masson SAS. All rights reserved.
http://dx.doi.org/10.1016/j.ejmech.2013.09.052

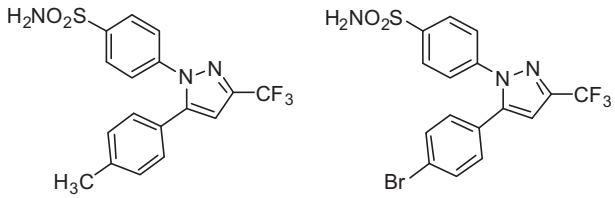

Fig. 1. Structures of celecoxib (left) and SC-588 (right).

the anti-inflammatory activity of a series of novel compounds: 1-(4,6-dimethylpyrimidin-2-yl)-5-hydroxy-5-trifluoromethyl-Δ^2-pyrazolines (3), 1-(4,6-dimethylpyrimidin-2-yl)-3-trifluoromethylpyrazoles (4) and 1-(4,6-dimethylpyrimidin-2-yl)-5-trifluoromethylpyrazoles (5), with the aim of finding new and more potent anti-inflammatory agents.

Moreover, considering that computer docking techniques play an important role in drug design as well as in mechanistic studies by placing a molecule into the binding site of the target macromolecule in a non covalent fashion, we have docked our compounds into the active site of COX-2 (PDB crystal structure: 3LN1 [19]). Our objective is to rationalize the potential as anti-inflammatory agents of these compounds by predicting their binding modes, binding affinities and optimal orientation at the active site of the COX-2 enzyme.

2. Results and discussion

2.1. Synthesis

Treatment of equimolar quantities of 2-hydrazino-4,6-dimethylpyrimidine (**1**) and methyl- (**2a**), trifluoromethyl- (**2b**) or 2-thienyltrifluoromethyl-β-diketones (**2c**) in ethanol resulted in the exclusive formation of 1-(4,6-dimethylpyrimidin-2-yl)-3-methyl- (**3a**), 3-trifluoromethyl- (**3b**) and 3-(2-thienyl)-5-hydroxy-5-trifluoromethyl-Δ^2-pyrazolines (**3c**) as depicted in Scheme 1.

However, similar treatment of compound **1** with aryltrifluoromethyl-β-diketones (**2d**–**h**, see Scheme 1) furnished two products: 1-(4,6-dimethylpyrimidin-2-yl)-3-aryl-5-hydroxy-5-trifluoromethyl-Δ^2-pyrazolines (**3d**–**h**) (major) and 1-(4,6-dimethylpyrimidin-2-yl)-5-aryl-3-trifluoromethylpyrazoles (**4d**–**h**) (minor). The products thus obtained were purified by column chromatography and their ratio was measured by means of the ^{1}H NMR spectra of the crude reaction mixtures (Table 1).

Presence of strong electron withdrawing CF_3 group at position 5 of pyrazolines **3a**–**h** makes them resistant to undergo dehydration under neutral conditions. Therefore, dehydration of **3a**–**h** to corresponding 5-trifluoromethylpyrazoles **5a**–**h** was achieved by treating them with acetic anhydride or EtOH–H_2SO_4. All the products have been unambiguously characterized by a combined application of ^{1}H, ^{13}C, ^{19}F NMR, mass spectra and elemental analyses.

The ^{1}H NMR spectra of compounds **3a**–**h** displayed two doublets of one proton intensity each at δ 3.74 ppm (J_{HA-HB} = 18 Hz) and at 3.62 ppm (J_{HA-HB} = 18 Hz) due to geminal coupling of the proton H_B with H_A of pyrazoline ring and vice-versa. This particular pattern is expected from two methylene protons (H_AH_B) (cis and trans to the CF_3 group, respectively) at position 4 of hydroxypyrazolines. The ^{1}H NMR spectra of compounds **4d**–**h** show a singlet of one proton intensity in the range δ 7.02–7.03 corresponding to position 4 of the pyrazole ring whereas this proton resonated at about δ 7.18–7.23 ppm in compounds **5a**–**h**, which is about 0.2 ppm downfield as compared to the corresponding proton in the regioisomers **4d**–**h**. Further, the ^{13}C NMR spectra of 5-hydroxypyrazolines **3a**–**h** confirmed the presence of the pyrazoline ring and those of compounds **4d**–**h** and **5a**–**h** corresponded to the aromatic pyrazole ring [17]. These values are in close agreement with the reported values for pyrazoline and isomeric pyrazole carbons 3, 4 and 5. The complete assignment of carbon signals of the compounds **3a**–**h**, **4d**–**h** and **5a**–**h** are given in the Supporting information. Finally, ^{19}F NMR spectra of compounds **3a**–**h** showed a signal in the range δ −81.29 to −82.45, which is characteristic for CF_3 bounded to a saturated carbon in accordance with the literature values [20,21]. In 3-trifluoromethylpyrazoles **4**, a sharp singlet appeared at about δ −63 ppm showing that CF_3 is bonded to double bond and located at position 3. However, in 5-trifluoromethylpyrazoles **5** CF_3 group present at position 5 showed a singlet at about δ −58 ppm in the ^{19}F NMR spectra (see Supporting information).

2.2. Anti-inflammatory activity

Fifteen of the compounds prepared (**3b**, **d**–**g**, **4d**–**h**, **5b**–**d**, **f**–**g**) were tested *in vivo* for their anti-inflammatory activity by the

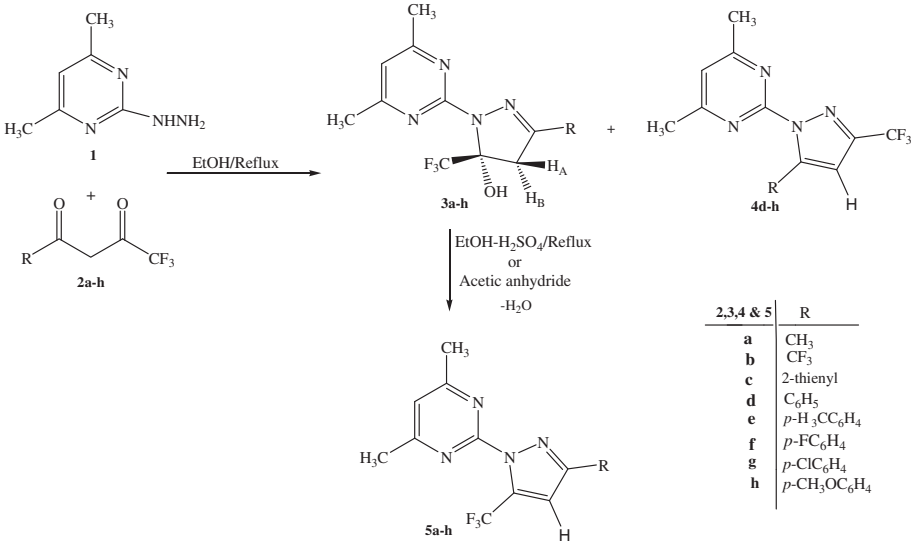

Scheme 1. Synthesis of title compounds **3**, **4** and **5**.

Table 1
Ratio of different products obtained as calculated by ^{1}H NMR of the crude reaction mixtures.

Compound	*a*	*b*	*c*	*d*	*e*	*f*	*g*	*h*
% **3**	100	100	100	57	55	74	64	53
% **4**	Nil	Nil	Nil	43	45	26	36	47

carrageenan-induced rat paw edema assay [22]. Each compound was dosed orally (50 mg kg^{-1} body weight) 30 min prior to induction of inflammation by carageenan injection. Indomethacin was utilized as the reference anti-inflammatory drug at a dose of 10 mg kg^{-1}. The anti-inflammatory activity was then calculated from 60 to 240 min after induction and presented in Table 2 as the mean paw volume (mL) in addition to the percentage anti-inflammatory activity (AI%).

A comparative study of the anti-inflammatory activity of the test compounds relative to the reference drug at different time intervals indicated that after 1 h, compounds **3f**, **4e**, **4g** and **4h** showed distinctive pharmacokinetic profiles as revealed from their potent and rapid onset of action with percentage activity of 42–56%. After 2 h, seven compounds (**3f**–**g**, **4e**–**h** and **5g**) showed good anti-inflammatory activity ranging from 50 to 64% as compared to indomethacin (75%). Taking anti-inflammatory activity after 3 h interval as a criterion for comparison (see Table 3), it can be concluded that while all the compounds showed potent anti-inflammatory activity (47–76%), compounds **4g** (76%) and **4h** (72%) exhibited excellent anti-inflammatory effect comparable with that of indomethacin (78%).

Compounds **3e**, **4d**–**h**, **5d** and **5g** displayed a good anti-inflammatory activity (50–63%) even after 4 h; however, none of them was found to be superior to the reference drug. The difference in anti-inflammatory activity found between 3-trifluoromethylpyrazoles (**4d**–**h**, AI 62–76%) and that of their analogs **4d**–**h** and **5a**–**h**, indicates that the location of trifluoromethyl group at position 3 of the pyrazole ring is playing a significant role on the anti-inflammatory activity as compared to the 5-trifluoromethyl compounds. This observation is strengthened by the fact that the commercial anti-inflammatory drugs such as celecoxib and SC-588 also possess a CF_3 group at position 3 of the pyrazole ring. Moreover, incorporation of substituents at the phenyl ring in compounds **4d**–**h** increases the anti-inflammatory activity from 62 to 76%. Pyrazolines **3a**–**h** and the corresponding pyrazoles **5a**–**h** showed similar level of anti-inflammatory activity thus indicating that dehydration of pyrazoline does not cause any remarkable effect.

3. Molecular modeling

With the aim to rationalize the good anti-inflammatory activity results obtained and taking into account that COX-2 is the most relevant enzymatic system for inflammation and the target of our compounds, a molecular modeling study was undertaken, by means of a combination of docking and molecular dynamics (MD) using the crystal structure of COX-2 (3NL1), with the compounds prepared and celecoxib as the reference ligand. The MOE 2011.10 modeling software (Molecular Operating Environment) was used for this study [23].

Each docking simulation was evaluated based on the London dG scores of generated poses after molecular mechanics refinement, which indicate the interaction energy between the ligand and the COX-2 binding site. The docking scores for the top ranked poses are presented in Table 3. It was notable that the majority of the poses, and all of those with good binding energies, were highly similar and it seems there is little room for extension in the binding site.

The geometries of the top ranked poses indicate that celecoxib and **4g** adopt very similar orientations in the binding site and interact with many of the same amino acid residues; this orientation is identical to that displayed by celecoxib in the crystal structure 3LN1. However, this is not the case for the remaining ligands **5g**, **3gR** and **3gS**, which are unable to adopt such a pose due to their linear geometry. An overlay of the top ranked docking pose of both celecoxib and **4g** demonstrates the similarities in their placement within the binding site (Fig. 2). Both ligands occupy the same space within the site and incorporate the same interaction with Ala513. Furthermore, in both poses the CF_3 group is placed within the same region of the binding site.

An analysis of the molecular surface created by the amino acid residues of the binding site and their hydrophilic/hydrophobic nature (Fig. 3, regions of pink and green represent hydrophilic and hydrophobic residues in the binding site, respectively) reveals several features. Firstly, the site is quite small and extension of the ligands would be unlikely to favor activity. Secondly, the geometry of both celecoxib and **4g** places the trifluoromethyl group in a highly hydrophobic region of the binding site (green surface), while **3gR**, **3gS** and **5g** force the trifluoromethyl group into a more

Table 2
Volume of edema (mL ± SEM) and anti-inflammatory activity (%AI, in brackets) of the compounds in the carrageenan-induced rat paw edema assay (acute inflammatory model).

Time	1 h	2 h	3 h	4 h
Control	0.69 ± 0.12	0.95 ± 0.01	1.89 ± 0.03**	1.94 ± 0.002
Indomethacin	0.21 ± 0.06** (69)	0.23 ± 0.02**(75)	0.41 ± 0.05** (78)	0.49 ± 0.01**(74)
3b	0.40 ± 0.01 (42)	0.53 ± 0.05 (44)	0.96 ± 0.10** (49)	1.49 ± 0.09 (23)
3d	0.38 ± 0.06 (44)	0.50 ± 0.09 (47)	0.94 ± 0.10** (50)	1.05 ± 0.25(45)
3e	0.47 ± 0.11(32)	0.62 ± 0.11(35)	0.86 ± 0.19** (54)	0.97 ± 0.16**(50)
3f	0.35 ± 0.02** (49)	0.45 ± 0.08** (51)	0.86 ± 0.10** (54)	1.19 ± 0.14 (38)
3g	0.65 ± 0.40 (5.7)	0.47 ± 0.11**(50)	0.76 ± 0.11** (59)	1.07 ± 0.01 (45)
4d	0.46 ± 0.04 (33)	0.54 ± 0.03 (43)	0.72 ± 0.11** (62)	0.95 ± 0.02** (51)
4e	0.36 ± 0.12** (48)	0.42 ± 0.01** (55)	0.58 ± 0.10** (69)	0.91 ± 0.08** (53)
4f	0.49 ± 0.06 (29)	0.46 ± 0.04** (59)	0.62 ± 0.01**(67)	0.81 ± 0.02** (58)
4g	0.31 ± 0.01** (55)	0.34 ± 0.05** (64)	0.49 ± 0.04** (76)	0.72 ± 0.24** (63)
4h	0.30 ± 0.12**(56)	0.38 ± 0.20** (59)	0.53 ± 0.12** (72)	0.76 ± 0.24**(61)
5b	0.45 ± 0.05 (34)	0.51 ± 0.04 (46)	0.81 ± 0.13** (57)	1.09 ± 0.01 (44)
5c	0.63 ± 0.13 (8.6)	0.78 ± 0.06 (18)	1.00 ± 0.20** (47)	1.22 ± 0.18 (37)
5d	0.66 ± 0.04 (4.3)	0.76 ± 0.03(20)	0.77 ± 0.02** (59)	0.84 ± 0.10** (56)
5f	0.51 ± 0.03 (26)	0.59 ± 0.08 (38)	0.85 ± 0.05** (55)	0.98 ± 0.11 (49)
5g	0.45 ± 0.02 (35)	0.57 ± 0.06**(54)	0.78 ± 0.03** (58)	0.91 ± 0.04** (53)

**Significantly different compared to respective control values, $P < 0.01$.Dose levels: test compounds (50 mg/kg body weight), Indomethacin (10 mg/kg body weight).

Table 3
Calculated docking scores (kcal mol^{-1}) for the top ranked poses of the docking of all compounds prepared in the crystal structure of COX-2 (3LN1). The docking score of the reference compound (celecoxib) is also included.

Substrate	E-refine
Celecoxib	−59.88
4g	−41.92
5g	−45.55
3gR	−49.77
3gS	−29.12

hydrophilic region of the site. As the trifluoromethyl group is thought to be a pharmacophoric feature for binding to the COX-2 receptor, its placement within the site is likely to be decisive for attaining high binding affinity ligands.

Taking celecoxib as the model system, and having decided that **4g** was the most suited ligand for the COX-2 binding site, MD simulations were carried out on the complexes of both ligands (see experimental section for all detailed procedures). Initially, top 10 ranked poses of both celecoxib and **4g** were relaxed in a 7 step minimization procedure to prepare the system for MD. The MMPBSA method for analyzing interaction energies [24], which includes aqueous solvation effects, was applied to these minimized structures (Table 4, MMPPBSA 1st Frame) and the most stable complex of each ligand was taken forward for MD. After heating from 0 to 300 K and equilibration of the systems, a production run of 10 ns was carried out on each complex. The MMPBSA method was then applied to probe the stability of the complexes over time.

The results from the MD study are shown in Table 4. The initial seven step minimization and MMPBSA 1st frame analysis was run for the five molecules. The 10 ns simulation was only run for celecoxib and **4g**. An analysis of the evolution of ΔG over the 10 ns of production MD, in which 500 snapshots were calculated, reveals that the system was more stabilized over the final 5 ns and so the values of ΔG quoted in Table 4 are for this period of the simulation. The values calculated with both the Generalised Born (GB) and Poisson Boltzmann (PB) solvation methods are provided.

The Δ*G* values for the minimized systems (ΔG 1st frame) reproduce the same order of interaction strength as the docking. Celecoxib shows the highest affinity by both methods. While **4g** was not the second highest affinity ligand, its pose best reproduced that of celecoxib. The higher affinity of **3gR**, **3gS** and **5g** can be attributed to the fact that the enzyme can adapt to their linear conformation, though it is unlikely that this is a favorable binding orientation at COX-2.

An analysis of the evolution of ΔG with time during the MD simulation (see Supporting information) reveals that the complexes are more stable in the 5–10 ns range and that **4g** was less stable in the COX-2 binding site than celcoxib since it took 2 ns to evolve to a stable complex and continued to show fluctuations in Δ*G* throughout. This is visible when the docking pose and average complex from 5 to 10 ns of each ligand are compared (Fig. 4). Celecoxib is maintained in the same position throughout the simulation, while **4g** had to rotate the pyrimidine-pyrazole bond to avoid steric strain induced by the methyl groups on the pyrimidine ring. This forces the pyrimidine ring to fill a different space in the receptor to the analogous phenyl ring of celecoxib.

Combining both modeling and biological results, it can be predicted that analogs of **4g** with reduced steric bulk at the 2- and 4-positions of the pyrimidine ring could have high affinity for the COX-2 binding site. This would maintain the CF_3 and chlorophenyl groups in similar regions of space to those of celecoxib and, furthermore, it opens up the possibility of new hydrogen bonding to the pyrimidine nitrogen, as suggested by the MD simulation.

4. Conclusion

In summary, three series of biologically active compounds 1-(4,6-dimethylpyrimidin-2-yl)-3-substituted-5-hydroxy-5-trifluoromethyl-Δ^2-pyrazolines (**3a**–**h**), 1-(4,6-dimethyl pyrimidin-2-yl)-5-substituted-3-trifluoromethylpyrazoles (**4d**–**h**) and 1-(4,6-dimethyl pyrimidin-2-yl)-3-substituted-5-trifluoromethylpyrazoles (**5a**–**h**) were synthesized by the condensation of 2-hydrazino-4,6-dimethylpyrimidine **1** with different trifluoromethyl-β-diketones (**2a**–**h**).

Fifteen of all the synthesized compounds were evaluated for their anti-inflammatory activity using the carrageenan-induced rat paw edema assay. Amongst the tested compounds **4g** (76%) and **4h** (72%) displayed excellent anti-inflammatory activity as compared to indomethacin (78%), whereas compounds **3e**, **4d**–**h**, **5d** and **5g** shown good anti-inflammatory activity (50–63%). 3-Trifluoromethylpyrazoles (**4d**–**h**) shown better anti-inflammatory activity than the corresponding regioisomeric 5-trifluoromethylpyrazoles (**5a**–**h**). Also, dehydration of the pyrazolines **3a**–**h** to the corresponding pyrazoles **5a**–**h** has negligible influence on the anti-inflammatory activity.

Docking experiments show that the compounds that better fit into the COX-2 active site are **4g**, **5g** and **3g** (both the R and S isomers) as compared with celecoxib. Further MD simulations including solvation effects indicate that compound **4g** adapts to the binding site explaining the good anti-inflammatory activity

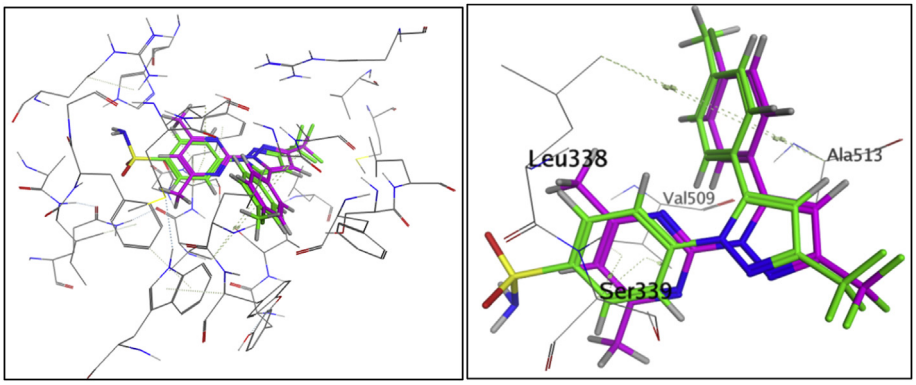

Fig. 2. Overlay of celecoxib (green) and **4g** (pink) top ranked docking pose in COX-2 binding site (*left*) and zoomed image showing interactions (*right*). Celecoxib interacts with Leu338, Ala513 and Ser339, while **4g** interacts with Val509 and Ala513. (For interpretation of the references to color in this figure legend, the reader is referred to the web version of this article.)

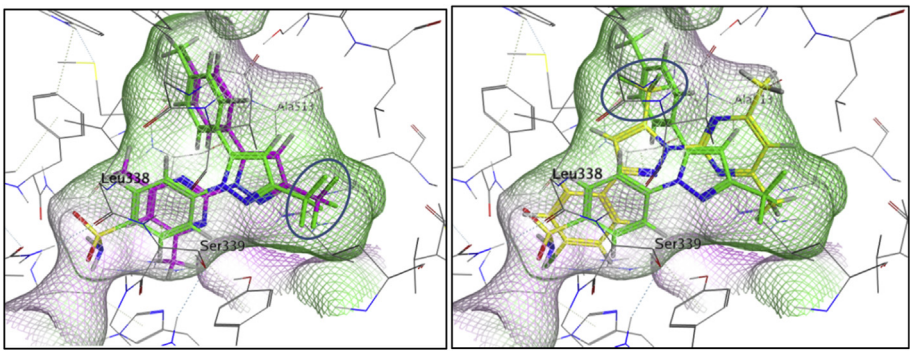

Fig. 3. Overlay of top ranked poses of celecoxib and **4g** (*left*) and celecoxib and **5g** (*right*). The CF_3 group (circled) of **4g** and celecoxib is placed in a hydrophobic region of binding site, whereas that of **5g** is forced into a more hydrophilic region of the site.

observed for this series in the carrageenan inflammation assay. These studies clearly indicate compound **4g** as a new lead compound that could drive to new and improved anti-inflammatory agents.

5. Experimental protocols

5.1. Synthesis

Melting points were determined in open capillaries and are uncorrected. IR spectra were recorded on a Buck Scientific IR M-500 spectrophotometer in KBr pellets, ^{1}H and ^{13}C NMR spectra for analytical purpose were recorded in $CDCl_3$ on a Bruker instrument at 300 MHz and 75 MHz, respectively; chemical shifts are expressed in δ-scale downfield from TMS as an internal standard. ^{19}F NMR spectra were run on DRX 300 and DPX 400 at 282 and 376 MHz, respectively, using deuteriochloroform as a solvent. The internal standard for ^{19}F spectra was fluorotrichloromethane, setting the $CFCl_3$ signal at δ 0.0. Elemental analyses were performed at the Central Drug Research Institute, Lucknow, India. Fluorinated β-diketones **2a**–**c** are available commercially and other **2d**–**h** were prepared according to literature procedure [25,26]. 2-Hydrazino-4,6-dimethylpyrimidine **1** was also synthesized according to literature procedure [27,28].

5.1.1. General procedure for the preparation of 1-(4,6-dimethylpyrimidin-2-yl)-5-hydroxy-5-trifluoromethyl-Δ^2-pyrazolines **3a**–**c**

An ethanolic solution (25 mL) of 2-hydrazino-4,6-dimethylpyrimidine **1** (0.27 g, 2 mmol) and trifluoromethyl-β-diketones **2a**–**c** (2 mmol) was refluxed for 7 h. The reaction was monitored by tlc. On completion of reaction, solvent was evaporated *in vacuo* and the solid obtained was recrystallized from ethanol. The tlc and ^{1}H NMR of the reaction mixture showed the formation of a single product **3a**–**c**.

Table 4
Free energy values (kcal mol^{-1}) calculated from the MD simulations of the complexes of COX-2 (3LN1) with celecoxib and compounds **4g**, **5g**, **3gR** and **3gS**.

	ΔGGB[a] 1st frame	ΔGPB[b] 1st frame	ΔGGB[a] 5–10 ns	ΔGPB[b] 5–10 ns
Cel	−58.31	−36.21	−51.88	−22.41
4g	−32.93	−28.93	−33.91	−30.33
5g	−35.25	−28.01		
3gR	−35.66	−25.99		
3gS	−35.46	−31.18		

[a] Generalized Born method.
[b] Poisson Boltzmann method.

5.1.1.1. 5-Hydroxy-3-methyl-1-(4,6-dimethylpyrimidin-2-yl)-5-trifluoromethyl-Δ^2-pyrazoline (**3a**).

Mp. 116–118 °C; Yield 73%; IR (KBr, cm^{-1}): 3350 (O–H); ^{1}H NMR (300 MHz, $CDCl_3$) δ: 2.15 (s, 3H, CH_3), 2.42 (s, 6H, 4′, 6′-CH_3), 3.17–3.23 (d, 1H, $^2J_{HA-HB}$ = 18 Hz, 4-H_B), 3.32–3.38 (d, 1H, $^2J_{HA-HB}$ = 18 Hz, 4-H_A), 6.59 (s, 1H, 5′-H), 8.36 (bs, 1H, 5-OH, exchangeable with D_2O); MS (EI) *m*/*z*: 275.1 [M + 1]$^+$. Anal. Calcd. for $C_{11}H_{13}F_3N_4O$: C, 48.18; H, 4.78; N, 20.43. Found: C, 47.95; H, 4.39; N, 20.79.

5.1.1.2. 5-Hydroxy-1-(4,6-dimethylpyrimidin-2-yl)-3,5-bis(trifluoromethyl)-Δ^2-pyrazoline (**3b**).

Mp. 80–82 °C; Yield 76%; IR (KBr, cm^{-1}): 3380 (O–H); ^{1}H NMR (300 MHz, $CDCl_3$) δ: 2.48 (s, 6H, 4′, 6′-CH_3), 3.35–3.46 (d, 1H, $^2J_{HA-HB}$ = 18 Hz, 4-H_B), 3.58–3.64 (d, 1H, $^2J_{HA-HB}$ = 18 Hz, 4-H_A), 6.77 (s,1H, 5′-H), 8.17 (bs, 1H, 5-OH, exchangeable with D_2O); MS(EI) *m*/*z*: 329.2 [M + 1]$^+$. Anal. Calcd. for $C_{11}H_{10}F_6N_4O$: C, 40.25; H, 3.07; N, 17.07. Found: C, 39.78; H, 2.79; N, 17.38.

5.1.1.3. 5-Hydroxy-3-(2-thienyl)-1-(4,6-dimethylpyrimidin-2-yl)-5-trifluoromethyl-Δ^2-pyrazoline (**3c**).

Mp. 182–184 °C; Yield 71%; IR (KBr, cm^{-1}): 3370 (O–H); ^{1}H NMR (300 MHz, $CDCl_3$) δ: 2.46 (s, 6H, 4′, 6′-CH_3), 3.61–3.68 (d, 1H, $^2J_{HA-HB}$ = 18 Hz, 4-H_B), 3.76–3.82 (d, 1H, $^2J_{HA-HB}$ = 18 Hz, 4-H_A), 6.64 (s, 1H, 5′-H), 7.07–7.10 (m, 1H, 4″-H), 7.30–7.31(m, 1H, 3″-H), 7.44–7.45 (d, 1H, 2″-H), 8.49 (bs, 1H, 5-OH, exchangeable with D_2O); MS (EI) *m*/*z*: 343.1 [M + 1]$^+$. Anal. Calcd. for $C_{14}H_{13}F_3N_4OS$: C, 49.12; H, 3.83; N, 16.37. Found: C, 49.07; H, 4.03; N, 16.99.

5.1.2. General procedure for the preparation of 1-(4,6-dimethylpyrimidin-2-yl)-5-hydroxy-5-trifluoromethyl-Δ^2-pyrazolines **3d**–**h** and 1-(4,6-dimethylpyrimidin-2-yl)-3-trifluoromethyl pyrazoles **4d**–**h**

An equimolar mixture of 2-hydrazino-4,6-dimethylpyrimidine **1** (0.27 g, 2 mmol) and aryltrifluoromethyl-β-diketones **2d**–**h** (2 mmol) was refluxed in ethanol (25 mL) for 7 h. The reaction was monitored by tlc. On completion of the reaction, solvent was evaporated *in vacuo*. The tlc and ^{1}H NMR of the reaction mixture showed the formation of two products in the ratio given in Table 1. Column chromatography separation using silica gel (100–200 mesh) with petroleum ether : ethyl acetate (99:1) as an eluent afforded **3** and further elution of column with petroleum ether : ethyl acetate (99:2) furnished the second product **4**.

5.1.2.1. 5-Hydroxy-3-phenyl-1-(4,6-dimethylpyrimidin-2-yl)-5-trifluoromethyl-Δ^2-pyrazoline (**3d**).

Mp. 154–156 °C; Yield 46%; IR (KBr, cm^{-1}) : 3365 (O–H); ^{1}H NMR (300 MHz, $CDCl_3$) δ: 2.47 (s, 6H, 4′, 6′-CH_3), 3.62–3.69 (d, 1H, $^2J_{HA-HB}$ = 18 Hz, 4-H_B), 3.76–3.82 (d, 1H, $^2J_{HA-HB}$ = 18 Hz, 4-H_A), 6.66 (s, 1H, 5′-H), 7.42–7.44 (m, 3H, 3″,

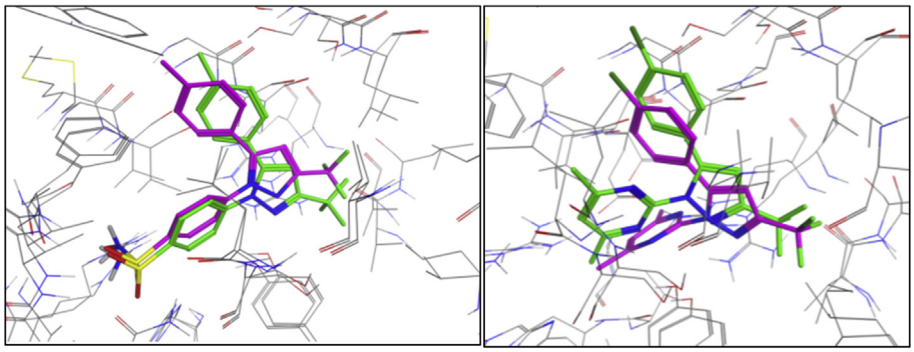

Fig. 4. Overlaid docking pose (green) and average structure from 5 to 10 ns of MD production (pink) for celecoxib (*left*) and **4g** (*right*). (For interpretation of the references to color in this figure legend, the reader is referred to the web version of this article.)

4″, 5″-H), 7.81–7.84 (m, 2H, 2″, 6″-H), 8.47 (bs, 1H, 5-OH, exchangeable with D_2O); MS (EI) *m/z*: 337.1 $[M + 1]^+$. Anal. Calcd. for $C_{16}H_{15}F_3N_4O$: C, 57.14; H, 4.50; N, 16.66. Found: C, 56.75; H, 4.81; N, 16.82.

*5.1.2.2. 5-Hydroxy-3-(4-methylphenyl)-1-(4,6-dimethylpyrimidin-2-yl)-5-trifluoromethyl-Δ²-pyrazoline (**3e**).* Mp. 134–136 °C; Yield 45%; IR (KBr, cm^{-1}): 3355 (O–H); ^1H NMR (300 MHz, $CDCl_3$) δ: 2.40 (s, 3H, 4″-CH_3), 2.46 (s, 6H, 4′, 6′-CH_3), 3.60–3.66 (d, 1H, $^2J_{HA–HB}$ = 18 Hz, 4-H_B), 3.74–3.80 (d, 1H, $^2J_{HA–HB}$ = 18 Hz, 4-H_A), 6.64 (s, 1H, 5′-H), 7.22–7.25 (d, 2H, *J* = 8.1 Hz, 3″, 5″-H), 7.69–7.72 (d, 2H, *J* = 8.1 Hz, 2″, 6″-H), 8.48 (bs, 1H, 5-OH, exchangeable with D_2O); MS (EI) *m/z*: 351.1 $[M + 1]^+$. Anal. Calcd. for $C_{17}H_{17}F_3N_4O$: C, 58.28; H, 4.89; N, 15.99. Found: C, 58.03; H, 5.12; N, 16.09.

*5.1.2.3. 5-Hydroxy-3-(4-fluorophenyl)-1-(4,6-dimethylpyrimidin-2-yl)-5-trifluoromethyl-Δ²-pyrazoline (**3f**).* Mp. 148–150 °C; Yield 58%; IR (KBr, cm^{-1}): 3365 (O–H); ^1H NMR (300 MHz, $CDCl_3$) δ: 2.47 (s, 6H, 4′, 6′-CH_3), 3.59–3.65 (d, 1H, $^2J_{HA–HB}$ = 18 Hz, 4-H_B), 3.73–3.79 (d, 1H, $^2J_{HA–HB}$ = 18 Hz, 4-H_A), 6.66 (s, 1H, 5′-H), 7.09–7.15 (m, 2H, 3″, 5″-H), 7.78–7.83 (m, 2H, 2″, 6″-H), 8.45 (bs, 1H, 5-OH, exchangeable with D_2O); MS (EI) *m/z*: 355.1 $[M + 1]^+$. Anal. Calcd. for $C_{16}H_{14}F_4N_4O$: C, 54.24; H, 3.98; N, 15.81. Found: C, 54.06; H, 4.23; N, 15.94.

*5.1.2.4. 5-Hydroxy-3-(4-chlorophenyl)-1-(4,6-dimethylpyrimidin-2-yl)-5-trifluoromethyl-Δ²-pyrazoline (**3g**).* Mp. 160–162 °C; Yield 54%; IR (KBr, cm^{-1}): 3355 (O–H); ^1H NMR (300 MHz, $CDCl_3$) δ: 2.47 (s, 6H, 4′, 6′-CH_3), 3.58–3.64 (d, 1H, $^2J_{HA–HB}$ = 18 Hz, 4-H_B), 3.72–3.79 (d, 1H, $^2J_{HA–HB}$ = 18 Hz, 4-H_A), 6.67 (s, 1H, 5′-H), 7.39–7.42 (d, 2H, *J* = 7.8 Hz, 3″, 5″-H), 7.74–7.76 (d, 2H, *J* = 7.8 Hz, 2″, 6″-H), 8.42 (bs, 1H, 5-OH, exchangeable with D_2O); MS (EI) *m/z*: 371.1/373.1 (3:1) $[M + 1]^+$/$[M + 1 + 2]^+$. Anal. Calcd. for $C_{16}H_{14}ClF_3N_4O$: C, 51.83; H, 3.81; N, 15.11. Found: C, 51.65; H, 3.98; N, 15.36.

*5.1.2.5. 5-Hydroxy-3-(4-methoxyphenyl)-1-(4,6-dimethylpyrimidin-2-yl)-5-trifluoromethyl-Δ²-pyrazoline (**3h**).* Mp. 150–152 °C; Yield 43%; IR (KBr, cm^{-1}): 3340 (O–H); ^1H NMR (300 MHz, $CDCl_3$) δ: 2.46 (s, 6H, 4′, 6′-CH_3), 3.59–3.65 (d, 1H, $^2J_{HA–HB}$ = 18 Hz, 4-H_B), 3.73–3.79 (d, 1H, $^2J_{HA–HB}$ = 18 Hz, 4-H_A), 3.86 (s, 3H, OCH_3), 6.63 (s, 1H, 5′-H), 6.93–6.96 (d, 2H, *J* = 8.7 Hz, 3″, 5″-H), 7.75–7.78 (d, 2H, *J* = 8.7 Hz, 2″, 6″-H), 8.50 (bs, 1H, 5-OH, exchangeable with D_2O); MS (EI) *m/z*: 367.1 $[M + 1]^+$. Anal. Calcd. for $C_{17}H_{17}F_3N_4O_2$: C, 55.74; H, 4.68; N, 15.29. Found: C, 55.23; H, 4.87; N, 15.67.

*5.1.2.6. 1-(4,6-Dimethylpyrimidin-2-yl)-5-phenyl-3-trifluoromethylpyrazole (**4d**).* Mp. 94–96 °C; Yield 34%; ^1H NMR (300 MHz, $CDCl_3$) δ: 2.60 (s, 6H, 4′, 6′-CH_3), 6.77 (s, 1H, 5′-H), 7.02 (s, 1H, 4-H), 7.32–7.36 (m, 3H, 3″, 4″, 5″-H), 7.99–8.02 (m, 2H, 2″, 6″-H); MS (EI) *m/z*: 319.1 $[M + 1]^+$. Anal. Calcd. for $C_{16}H_{13}F_3N_4$: C, 60.37; H, 4.12; N, 17.60. Found: C, 60.09; H, 4.03; N, 17.68.

*5.1.2.7. 1-(4,6-Dimethylpyrimidin-2-yl)-5-(4-methylphenyl)-3-trifluoromethylpyrazole (**4e**).* Mp. 96–98 °C; Yield 37%; ^1H NMR (300 MHz, $CDCl_3$) δ: 2.45 (s, 3H, 4″-CH_3), 2.61 (s, 6H, 4′, 6′-CH_3), 6.77 (s, 1H, 5′-H), 7.02 (s, 1H, 4-H), 7.36–7.38 (d, 2H, *J* = 8.1 Hz, 3″, 5″-H), 7.89–7.92 (d, 2H, *J* = 8.1 Hz, 2″, 6″-H); MS (EI) *m/z*: 333.1 $[M + 1]^+$. Anal. Calcd. for $C_{17}H_{15}F_3N_4$: C, 61.44; H, 4.55; N, 16.86. Found: C, 61.28; H, 4.62; N, 16.96.

*5.1.2.8. 1-(4,6-Dimethylpyrimidin-2-yl)-5-(4-fluorophenyl)-3-trifluoromethylpyrazole (**4f**).* Mp. 100–102 °C; Yield 21%; ^1H NMR (300 MHz, $CDCl_3$) δ: 2.43 (s, 6H, 4′, 6′-CH_3), 6.74 (s, 1H, 5′-H), 7.03 (s, 1H, 4-H), 7.08–7.14 (d, 2H, *J* = 8.1 Hz, 3″, 5″-H), 7.18–7.24 (d, 2H, *J* = 8.1 Hz, 2″, 6″-H); MS (EI) *m/z*: 337.1 $[M + 1]^+$. Anal. Calcd. for $C_{16}H_{12}F_4N_4$: C, 57.15; H, 3.60; N, 16.66. Found: C, 57.25; H, 3.75; N, 16.82.

*5.1.2.9. 1-(4,6-Dimethylpyrimidin-2-yl)-5-(4-chlorophenyl)-3-trifluoromethylpyrazole (**4g**).* Mp. 106–108 °C; Yield 30%; ^1H NMR (300 MHz, $CDCl_3$) δ: 2.44 (s, 6H, 4′, 6′-CH_3), 6.76 (s, 1H, 5′-H), 7.03 (s, 1H, 4-H), 7.20–7.23 (d, 2H, *J* = 8.4 Hz, 3″, 5″-H), 7.32–7.35 (d, 2H, *J* = 8.4 Hz, 2″, 6″-H); MS (EI) *m/z*: 353/355 (3:1) $[M + 1]^+$/$[M + 1 + 2]^+$. Anal. Calcd. for $C_{16}H_{12}ClF_3N_4$: C, 54.48; H, 3.43; N, 15.88. Found: C, 54.22; H, 3.56; N, 16.04.

*5.1.2.10. 1-(4,6-Dimethylpyrimidin-2-yl)-5-(4-methoxyphenyl)-3-trifluoromethylpyrazole (**4h**).* Mp. 98–100 °C; Yield 38%; ^1H NMR (300 MHz, $CDCl_3$) δ: 2.45 (s, 6H, 4′, 6′-CH_3), 3.84 (s, 3H, OCH_3), 6.71 (s, 1H, 5′-H), 6.85–6.88 (d, 2H, *J* = 8.4 Hz, 3″, 5″-H), 7.03 (s, 1H, 4-H), 7.19–7.21 (d, 2H, *J* = 8.4 Hz, 2″, 6″-H); MS (EI) *m/z*: 349.1 $[M + 1]^+$. Anal. Calcd. for $C_{17}H_{15}F_3N_4O$: C, 58.62; H, 4.34; N, 16.08. Found: C, 58.36; H, 4.58; N, 16.32.

*5.1.3. General procedure for the preparation of 1-(4,6-dimethylpyrimidin-2-yl)-5-trifluoromethylpyrazoles **5a–h***

1-(4,6-Dimethylpyrimidin-2-yl)-3-substituted-5-hydroxy-5-trifluoromethylpyrazolines **3** were dehydrated by refluxing in acetic anhydride 20 mL (as solvent) for 4 h. The reaction was monitored by tlc. On completion reaction mixture was poured into ice cold water and then filtered to give the required product **5**.

*5.1.3.1. 1-(4,6-Dimethylpyrimidin-2-yl)-3-methyl-5-trifluoromethylpyrazole (**5a**).* Mp. 92–94 °C; Yield 79%; ^1H NMR (300 MHz, $CDCl_3$) δ: 2.41 (s, 3H, CH_3), 2.56 (s, 6H, 4′, 6′-CH_3), 6.70 (s, 1H, 5′-H), 7.00 (s, 1H, 4-H); MS (EI) *m/z*: 257.1 $[M + 1]^+$. Anal. Calcd.

for $C_{11}H_{11}F_3N_4$: C, 51.56; H, 4.33; N, 21.87. Found: C, 51.38; H, 4.56; N, 22.15.

*5.1.3.2. 1-(4,6-Dimethylpyrimidin-2-yl)-3,5-bis(trifluoromethyl)pyrazole (**5b**).* Mp. 70–72 °C; Yield 69%; ^{1}H NMR (300 MHz, $CDCl_3$) δ: 2.59 (s, 6H, 4′, 6′-CH_3), 7.09 (s, 1H, 5′-H), 7.11 (s, 1H, 4-H); MS (EI) *m/z*: 311.1 $[M + 1]^+$. Anal. Calcd. for $C_{11}H_8F_6N_4$: C, 42.59; H, 2.60; N, 18.06. Found: C, 42.47; H, 2.77; N, 18.35.

*5.1.3.3. 1-(4,6-Dimethylpyrimidin-2-yl)-3-(2-thienyl)-5-trifluoromethylpyrazole (**5c**).* Mp. 120–122 °C; Yield 78%; ^{1}H NMR (300 MHz, $CDCl_3$) δ: 2.53 (s, 6H, 4′, 6′-CH_3), 6.97 (s, 1H, 5′-H), 7.02 (m, 1H, 4″-H), 7.20 (s,1H, 4-H), 7.27–7.29 (m, 1H, 3″-H), 7.42–7.44 (m, 1H, 2″-H); MS (EI) *m/z*: 325.1 $[M + 1]^+$. Anal. Calcd. for $C_{14}H_{11}F_3N_4S$: C, 51.85; H, 3.42; N, 17.27. Found: C, 51.65; H, 3.73; N, 17.98.

*5.1.3.4. 1-(4,6-Dimethylpyrimidin-2-yl)-3-phenyl-5-trifluoromethylpyrazole (**5d**).* Mp. 101–103 °C; Yield 36%; ^{1}H NMR (300 MHz, $CDCl_3$) δ: 2.61 (s, 6H, 4′, 6′-CH_3), 7.07 (s, 1H, 5′-H), 7.23 (s, 1H, 4-H), 7.37–7.49 (m, 3H, 3″, 4″, 5″-H), 7.94–7.96 (m, 2H, 2″, 6″-H); MS (EI) *m/z*: 319.1 $[M + 1]^+$. Anal. Calcd. for $C_{16}H_{13}F_3N_4$: C, 60.37; H, 4.12; N, 17.60. Found: C, 60.09; H, 4.03; N, 17.68.

*5.1.3.5. 1-(4,6-Dimethylpyrimidin-2-yl)-3-(4-methylphenyl)-5-trifluoromethylpyrazole (**5e**).* Mp. 112–114 °C; Yield 28%; ^{1}H NMR (300 MHz, $CDCl_3$) δ: 2.41 (s, 3H, 4″-CH_3), 2.61 (s, 6H, 4′, 6′-CH_3), 7.06 (s, 1H, 5′-H), 7.20 (s, 1H, 4-H), 7.25–7.28 (d, 2H, J = 8.1 Hz, 3″, 5″-H), 7.83–7.86 (d, 2H, J = 8.1 Hz, 2″, 6″-H); MS (EI) *m/z*: 333.1 $[M + 1]^+$. Anal. Calcd. for $C_{17}H_{15}F_3N_4$: C, 61.44; H, 4.55; N, 16.86. Found: C, 61.28; H, 4.62; N, 16.96.

*5.1.3.6. 1-(4,6-Dimethylpyrimidin-2-yl)-3-(4-fluorophenyl)-5-trifluoromethylpyrazole (**5f**).* Mp. 114–116 °C; Yield 32%; ^{1}H NMR (300 MHz, $CDCl_3$) δ: 2.62 (s, 6H, 4′, 6′-CH_3), 7.08 (s, 1H, 5′-H), 7.12–7.15 (m, 2H, 3″, 5″-H), 7.18 (s, 1H, 4-H),7.90–7.95 (m, 2H, 2″, 6″-H); MS (EI) *m/z*: 337.1 $[M + 1]^+$. Anal. Calcd. for $C_{16}H_{12}F_4N_4$: C, 57.15; H, 3.60; N, 16.66. Found: C, 57.25; H, 3.75; N, 16.82.

*5.1.3.7. 1-(4,6-Dimethylpyrimidin-2-yl)-3-(4-chlorophenyl)-5-trifluoromethylpyrazole (**5g**).* Mp. 126–128 °C; Yield 40%; ^{1}H NMR (300 MHz, $CDCl_3$) δ: 2.61 (s, 6H, 4′, 6′-CH_3), 7.09 (s, 1H, 5′-H), 7.20 (s, 1H, 4-H), 7.42–7.44 (d, 2H, J = 8.1 Hz, 3″, 5″-H), 7.88–7.90 (d, 2H, J = 8.1 Hz, 2″, 6″-H); MS (EI) *m/z*: 353/355 (3:1) $[M + 1]^+$/$[M + 1 + 2]^+$. Anal. Calcd. for $C_{16}H_{12}ClF_3N_4$: C, 54.48; H, 3.43; N, 15.88. Found: C, 54.22; H, 3.56; N, 16.04.

*5.1.3.8. 1-(4,6-Dimethylpyrimidin-2-yl)-3-(4-methoxyphenyl)-5-trifluoromethylpyrazole (**5h**).* Mp. 108–110 °C; Yield 28%; ^{1}H NMR (300 MHz, $CDCl_3$) δ: 2.63 (s, 6H, 4′, 6′-CH_3), 3.86 (s, 3H, OCH_3), 6.92–6.95 (d, 2H, J = 8.4 Hz, 3″, 5″-H), 7.03 (s, 1H, 5′-H), 7.41 (s, 1H, 4-H), 7.81–7.84 (d, 2H, J = 8.4 Hz, 2″, 6″-H); MS (EI) *m/z*: 349.1 $[M + 1]^+$. Anal. Calcd. for $C_{17}H_{15}F_3N_4O$: C, 58.62; H, 4.34; N, 16.08. Found: C, 58.36; H, 4.58; N, 16.32.

5.2. Pharmacological assay

The protocol of animal experiments has been approved by the Institutional Animal Ethics Committee (IAEC). Male Wister albino rats weighing 200–250 g were used throughout the study. They were kept in the animal house under standard conditions of light and temperature with free access to food and water. Food was withdrawn 12 h before and during experimental hours. The animals were randomly divided into groups each consisting of six rats. One group of six rats was kept as control and received tween 80 (95:5). Another group received the standard drug indomethacin at a dose of 10 mg/kg body weight, p.o.. Other groups of rats were administered the test compounds at a dose of 50 mg/kg body weight orally. A mark was made on the left hind paw just beyond the tidiotarsal articulation, so that every time the paw was dipped up to fixed mark and constant paw volume was ensured. Paw volumes were measured using a plethsymometer (model 7140, UgoBasile, Italy). Thirty minutes after administration of test and standard drugs, 0.1 mL of 1% w/v of carrageenan suspension in normal saline was injected into subplanter region of the left hind paw of all the animals. The initial paw volume was measured within 30 s of the injection and remeasured again 1 h, 2 h, 3 h and 4 h after administration of carrageenan. The anti-inflammatory effect of ethanolic extract was calculated by the following equation:

$$\text{Anti} - \text{inflammatory activity}(\%) = (V_c - V_t/V_c) \times 100$$

where V_t represents the paw volume in drug treated animals and V_c represents the paw volume of control group of animals.

5.3. Molecular docking methodology

5.3.1. Preparation of input structures for docking and molecular dynamics

The crystal structure of celecoxib bound at the *musmusculus* COX-2 active site (3LN1) [19] was imported into the MOE 2011.10 modeling software (Molecular Operating Environment) [23]. As the receptor consists of four identical domains – each binding a celecoxib molecule – three of these chains were removed, along with water molecules and other small molecules (HEM, NAG, BOG). The structure was protonated using the Protonate 3D tool in MOE applying the default parameters.

The structures of celecoxib, **3g** (R and S enantiomers), **4g** and **5g** ligands were built in MOE. They were minimized using the MMFF94× force field with 0.05 gradient, and a full conformational search was conducted using the Low ModeMD [29] method with a minimum of 100 iterations.

The conformers generated were docked into the COX-2 receptor using the triangle matcher placement method and the London dG scoring function. A molecular mechanics force field refinement was carried out on the top 30 poses generated in which side chains were free to move and a non-interacting cutoff of 12 Å was applied.

The 10 top ranked poses from docking were saved as separate pdb files. Each complex was then converted into an Amber structure file using tLEAP. Force field parameters and partial charges from the ff99sb force field were applied for the protein, while the ligands were prepared using the general amber force field (GAFF) parameter assignment [30] in the antechamber program implemented in Amber version 11 [31]. Each complex was placed in a TIP3P [32] water box, keeping the minimum distance between the protein and the walls of the box to 12 Å. Three Na^+ counterions were added to the solvent bulk of protein/water with tLEAP to neutralize the system for MD simulations.

5.3.2. Molecular dynamics simulation protocol

The MD simulations were performed in the AMBER 11 software package. The solvated systems were minimized in a multistep procedure consisting of seven steps with reducing constraints on the system. In the first three steps, the steepest descent method was applied for 1000 steps, followed by 4000 steps of conjugate gradient, while restraining the protein backbone with a harmonic potential of force constant 50, 5, and 0.5 kcal mol^{-2} Å^{-2}, respectively. In the last steps, complexes were minimized without restrictions until the root-mean-square gradient of the potential energy was $\leq$0.001 kcal mol^{-1}. The MMPBSA approach was applied

to the conformation after the seventh minimization step for each of the 10 docked poses, providing generalized Born (GB) and Poisson-Boltzmann (PB) energy binding values.

The most stable complex for both Cel and **4g** were then heated in the NVT ensemble (constant volume and temperature conditions) from 0 to 300 K over 200 ps. The systems were equilibrated for 50ps at a constant temperature of 300 K by coupling the system to a thermal bath with the Berendsen [33] algorithm, a time coupling constant of 1 ps, and a pressure of 1 atm (NPT). The SHAKE [34] algorithm was used to constrain the bonds involving hydrogen atoms to their equilibrium values. A 10ns production run in the NVT ensemble at a constant temperature of 300 K was then applied by coupling the system to a thermal bath with the Berendsen algorithm and a time coupling constant of 2 ps. System convergence was evaluated through evolution of ΔG binding energies during the last 5 ns of simulation time.

5.3.3. MM-PB/GBSA approach

Binding free energy calculations were performed using the molecular mechanics Poisson-Boltzmann/Generalised Born surface area (MM-PB/GBSA) [24] implemented in Amber 11. A total of 500 snapshots were extracted from the last 5 ns of the trajectory for the calculations.

Acknowledgments

We (RA and IR) thank the Department of Science and Technology, New Delhi, India and University of Dublin, Trinity College, Dublin, Ireland for providing financial assistance under the India-Ireland Cooperative Science Program. AB is thankful to the Council of Scientific and Industrial Research, New Delhi for Senior Research Fellowship. BK is thankful to the HEA-PRTLI-4 program for financial support. Thanks are also due to the Mass Spectrometry Facility, University of California, San Francisco, USA for running the mass spectra.

Appendix A. Supplementary data

Supplementary data related to this article can be found at http://dx.doi.org/10.1016/j.ejmech.2013.09.052.

References

[1] G.Y. Chen, G. Nunez, Nat. Rev. Immunol. 10 (2010) 826–837.
[2] R. Medzhitov, Cell 140 (2010) 771–776.
[3] M.B. Goldring, M. Otero, Curr. Opin. Rheumatol. 23 (2011) 471–478.
[4] N. Herrmann, S.A. Chau, I. Kircanski, K.L. Lanctot, Drugs 71 (2011) 2031–2065.
[5] L. Minghetti, J. Neuropathol. Exp. Neurol. 63 (2004) 901–910.
[6] T.D. Penning, J.J. Talley, S.R. Bertenshaw, J.S. Carter, P.W. Collins, S. Docter, M.J. Graneto, L.F. Lee, J.W. Malecha, J.M. Miyashiro, R.S. Rogers, D.J. Rogier, S.S. Yu, G.D. Anderson, E.G. Burton, J.N. Cogburn, S.A. Gregory, C.M. Coboldt, W.E. Perkins, K. Seibert, A.W. Veenhuizen, Y.Y. Zhang, P.C. Isakson, J. Med. Chem. 40 (1997) 1347–1365.
[7] B.P. Bandgar, S.S. Gawande, R.G. Bodade, N.M. Gawande, N.C. Khobragade, Bioorg. Med. Chem. 17 (2009) 8168–8173.
[8] P. Rani, V.K. Srivastava, A. Kumar, Eur. J. Med. Chem. 39 (2004) 449–452.
[9] E. Bansal, V.K. Srivastava, A. Kumar, Eur. J. Med. Chem. 36 (2001) 81–92.
[10] R. Filler, Y. Kobayashi, Biomedicinal Aspects of Fluorine Chemistry, Elsevier, New York, 1982.
[11] M. Lindvall, C. McBride, M. McKenna, T.G. Gesner, A. Yabannavar, K. Wong, S. Lin, A. Walter, C.M. Shafer, Med. Chem. Lett. 2 (2011) 720–723.
[12] T.P. Heffron, M. Berry, G. Castanedo, et al., Bioorg. Med. Chem. Lett. 20 (2010) 2408–2411.
[13] N.S. Shetty, R.S. Lamani, I.M. Khazi, J. Chem. Sci. 121 (2009) 301–307.
[14] A.B.A. El-gazzar, H.A.R. Hussein, H.N. Hafez, Acta Pharm. 57 (2007) 395–411.
[15] V. Kumar, R. Aggarwal, S.P. Singh, Heterocycles 75 (2008) 2893–2929.
[16] S.P. Singh, V. Kumar, R. Aggarwal, J. Elguero, J. Heterocycl. Chem. 43 (2006) 1003–1014.
[17] R. Aggarwal, R. Kumar, S.P. Singh, J. Fluorine Chem. 130 (2009) 886–893.
[18] R. Aggarwal, R. Kumar, S. Kumar, G. Garg, R. Mahajan, J. Sharma, J. Fluorine Chem. 132 (2011) 965–972.
[19] J.L. Wang, D. Limburg, M.J. Graneto, J. Springer, J.R. Hamper, S. Liao, J.L. Pawlitz, R.G. Kurumbail, T. Maziasz, J.J. Talley, J.R. Kiefer, J. Carter, Bioorg. Med. Chem. Lett. 20 (2010) 7159–7163.
[20] V. Kumar, S.P. Singh, R. Aggarwal, J. Fluorine Chem. 127 (2006) 880–888.
[21] S.P. Singh, D. Kumar, B.G. Jones, M.D. Threadgill, J. Fluorine Chem. 94 (1999) 199–203.
[22] C.A. Winter, E.A. Risley, G.W. Nuss, Proc. Soc. Exp. Biol. Med. 111 (1962) 544–547.
[23] MOE. 2011.10, Chemical Computing Group, Montreal, 2011. www.chemcomp.com.
[24] P.A. Kollman, I. Massova, C. Reyes, B. Kuhn, S. Huo, L. Chong, M. Lee, T. Lee, Y. Duan, W. Wang, O. Donini, P. Cieplak, J. Srinivasan, D.A. Case, T.E. Cheatham, Acc. Chem. Res. 33 (2000) 889–897.
[25] M.J. Uddin, P.N. Rao, K. Praveen, E.E. Knaus, Bioorg. Med. Chem. 11 (2003) 5273–5280.
[26] K.T. Potts, J. Bhattacharya, S.L. Smith, A.M. Ihrig, C.A. Girard, J. Org. Chem. 37 (1972) 4410–4415.
[27] M.P.V. Boarland, J.F.W. McOmie, R.N. Timms, J. Chem. Soc. (1952) 4691–4694.
[28] G.G. Danagulyan, N.G. Balasanyan, P.B. Terent'ev, M.G. Zalinyan, Chem. Heterocyclic Compounds, New York, United State. 25 (12) (1989) 1369–1373. KhimiyaGeterotsiklicheskikhSoedinenii, 12 (1989) 1644–1648.
[29] P. Labute, J. Chem. Inf. Model 50 (2010) 792–800.
[30] D.A. Case, T.E. Cheatham III, T. Darden, H. Gohlke, R. Luo, K.M. Merz Jr., A. Onufriev, C. Simmerling, B. Wang, R.J. Woods, J. Comput. Chem. 26 (2005) 1668–1688.
[31] J. Wang, R.M. Wolf, J.W. Caldwell, P.A. Kollman, D.A. Case, J. Comput. Chem. 25 (2004) 1157–1174.
[32] W.L. Jorgensen, J. Chandrasekhar, J.D. Madura, R.W. Impey, M.L. Klein, J. Chem. Phys. 79 (1983) 926–935.
[33] H.J.C. Berendsen, J.P.M. Postma, W.F. Vangunsteren, A. Dinola, J.R. Haak, J. Chem. Phys. 81 (1984) 3684–3690.
[34] J.P. Ryckaert, G. Ciccotti, H.J.C. Berendsen, J. Comp. Physiol. 23 (1977) 327–341.